standard in 5 mL of chloroform and determining the oxidation products by GLC as reported above.

The identity and purity of the peroxidic oxidants were determined by elemental analysis, IR spectra, and iodometric titrations. Gas chromatographic analyses of reaction mixtures were carried out on a Perkin-Elmer 8420 gas chromatograph equipped with a flame ionization detector and program capability. GC–MS analyses were performed by a Hewlett-Packard Model 5890 gas chromatograph (using an HP-1 dimethylpolysiloxane 25 mt capillary column), equipped with a Hewlett-Packard MS computerized system, Model 5971A, ionization voltage 70

eV, electron multiplier 1700 V, ion source temperature 280 °C.

^{1}H NMR spectra were recorded on a Bruker WP-80 spectrometer with TMS as internal standard.

Oxidation products were identified by comparison of their MS and NMR spectra with those of authentic samples.

Diffusion and Percolation of Radical Pairs in Zeolite Media. A Product Analysis Study

Miguel A. Garcia-Garibay, Zhenyu Zhang,[†] and Nicholas J. Turro*

Contribution from the Department of Chemistry, Columbia University, New York, New York 10027. Received January 30, 1991. Revised Manuscript Received April 12, 1991

Abstract: The photochemistry of dibenzyl-d_5 ketone (DBK-d_5) adsorbed in the zeolite NaX was investigated as a function of substrate loading. The cage effect and the relative yields of 1,2-diphenylethane (DPE), o-methyl-β-phenylacetophenone (o-MAP), and p-methyl-β-phenylacetophenone (p-MAP) were found to depend dramatically on the loading of the starting material present. These results and the variations observed in the percent cage effect are described in terms of local and global effects that determine the influence of the zeolite media. Changes in reactivity as a function of reactant loading are explained in terms of percolation theory by using the model "ants in a labyrinth" proposed by de Gennes. The diffusing radicals play the role of the ants and the disposition of the reactant in the regular zeolite topology determines the nature of the labyrinth. This model implies that the diffusion coefficient of the radicals is larger than the diffusion coefficient of the starting ketone. The model is supported by trapping experiments with an oxygen scavenger and by experiments carried out at -20 °C where the diffusion of the radicals is largely diminished.

Introduction

Zeolites are microporous crystalline materials possessing molecular-sized and geometrically well defined interconnecting channels and cavities.[1] The adsorption and intracrystalline diffusion of organic compounds with kinetic diameters smaller than those of the critical zeolite dimensions give zeolites their sieving abilities. While the use of zeolites as active reaction catalysts has been well studied over the last few decades,[2] their properties as organizing reaction media for photochemical reactions have been explored only recently.[3-5] It has been shown, however, that both unimolecular[3] and bimolecular[4] photochemical reactions can be influenced by the structural arrangement and restrictions imposed on the reactants by the zeolite environment.

Local and Global Effects. The selectivity of photochemical reactions in zeolites is often very different than that observed in solution.[3-5] Unimolecular effects usually result from conformational restrictions[3] giving rise to reactant and transition-state selectivity control.[2] Bimolecular reactions, in contrast, depend on the distribution and transport of the reactants within the various sites of the zeolite environment.[4] Interestingly, these factors can be drastically influenced by relatively simple experimental manipulations such as ion exchange[6] and the use of small amounts of unreactive additives.[7] Recent photochemical investigations have demonstrated some of these effects on the product distribution of radical-mediated reactions.[4-6,8] In these particular cases, both the size/shape and binding interactions with the local environment as well as the connectivity of the internal zeolite channels may induce specific effects on the dynamics of recombinant radicals and radical pairs. Cage effects may originate at *locally* restricted sites where escape of the geminate radical pairs may be unfavorable, or within the *global* spaces given by extended and interconnected intracrystalline pore structures.[9] A distinction

between these two possibilities is of significant interest in order to understand the mechanisms that control chemical reactivity in these media. Local effects are expected to result from isolated reactant–zeolite site interactions, while global effects, involving diffusion and molecular transport, are expected to depend on the distribution of the reactants and be susceptible to cooperative interactions and critical phenomena. Local effects should be independent of the amount of reactant present in the zeolite, while global effects should depend on the amount of material present and its distribution in the intracrystalline reaction spaces. Here we report an investigation addressing the relative importance of local and global effects in a model system. With this in mind,

(1) Breck, D. W. *Zeolite Molecular Sieves*; John Wiley & Sons: New York, 1974.

(2) (a) Holderich, W.; Hesse, M.; Naumann, F. *Angew. Chem., Int. Ed. Engl.* **1988**, *27*, 226. (b) Ramoa Ribeiro, F., Rodrigues, A. E., Rollman, L. D., Naccache, C., Eds. *Zeolites: Science and Technology*; NATO ASI Series E, Appl. Sci. No. 80; The Hague, 1984. (c) Maxwell, I. E. *J. Inclusion Phenom.* **1986**, *4*, 1. (d) Csicery, S. M. *Pure Appl. Chem.* **1986**, *58*, 1986.

(3) Wilkinson, F.; Casal, H. L.; Johnston, L. J.; Scaiano, J. C. *Can. J. Chem.* **1986**, *64*, 539 and references therein.

(4) (a) Liu, X.; Iu, K.-K.; Thomas, J. K. *J. Phys. Chem.* **1989**, *93*, 4120. (b) Barretz, B. H.; Turro, N. J. *J. Photochem.* **1984**, *24*, 201. (c) Ramamurthy, V.; Corbin, D. R.; Kumar, C. V.; Turro, N. J. *Tetrahedron Lett.* **1990**, *31*, 47. (d) Mandeville, J. B.; Golub, J.; Kozak, J. J. *J. Phys. Chem.* **1988**, *92*, 1575.

(5) (a) Turro, N. J.; Wan, P. *J. Am. Chem. Soc.* **1985**, *107*, 678. (b) Turro, N. J. *Pure Appl. Chem.* **1986**, *58*, 1219.

(6) Turro, N. J.; Zhang, Z. *Tetrahedron Lett.* **1987**, *28*, 5517.

(7) (a) Turro, N. J.; Cheng, C.-C.; Lei, X.-G. *J. Am. Chem. Soc.* **1985**, *107*, 3739. (b) Turro, N. J.; Cheng, C.-C.; Abrahms, L.; Corbin, D. *J. Am. Chem. Soc.* **1987**, *109*, 2449. (d) Ramamurthy, V.; Caspar, J. V.; Corbin, D. R.; Eaton, D. F. *J. Photochem. Photobiol., A* **1989**, *50*, 157. (e) Ramamurthy, V.; Caspar, J. V.; Corbin, D. R. *J. Am. Chem. Soc.* **1991**, *113*, 594. (f) Caspar, J. V.; Ramamurthy, V.; Corbin, D. R. *J. Am. Chem. Soc.* **1991**, *113*, 600.

(8) Ghatlia, N. D.; Turro, N. J. *J. Photochem. Photobiol., A* **1991**, *57*, 7.

(9) Turro, N. J.; Garcia-Garibay, M. In *Photochemistry in Organized Media*; Ramamurthy, V., Ed., in press.

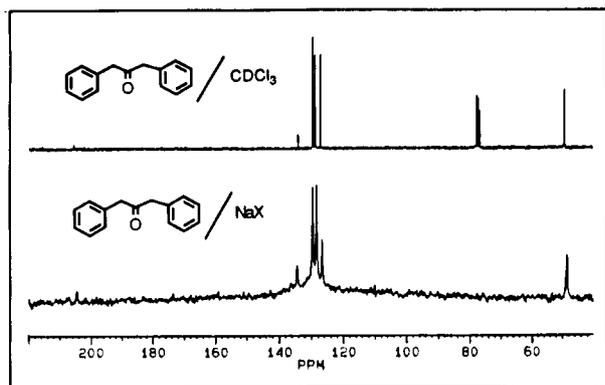†Present address: Inrad, Inc., 181 Legrand Ave., Northvale, NJ 07647.

Scheme I

we have studied the effects of reactant loading on the recombination reactions of radicals derived from dibenzyl ketone (DBK) in the zeolite NaX. It is shown here that radical recombination reactions are susceptible to loading effects in the system under study. This behavior may be understood qualitatively in terms of radical transport and percolation in the zeolite pore lattice under consideration.

Experimental Section

A sample of $C_6H_5CH_2COCH_2C_6D_5$ (DBK-d_5, Scheme I) was obtained by deuterium exchange of $C_6H_5CH_2COCD_2C_6D_5$, prepared and purified according to literature procedures.[10] Samples of 20–40 mg of zeolite NaX (Si/Al = 1.2) obtained from Union Carbide were calcined in a shallow bed at open air for 12 h at 550 °C and allowed to cool down to room temperature before exposure to DBK or DBK-d_5. The average crystal size indicated by the manufacturer is between 2.0 and 4.5 μm. Commercial solvents of the highest purity available were used for zeolite loading and extraction procedures. The amounts of ketone adsorbed in the zeolite phase from pentane solutions of known concentrations were determined spectrophotometrically (UV) at 220 nm in uptake rate measurements and adsorption isotherm studies.[1] The equilibrium concentration of DBK-d_5 in the pentane supernatant was determined after no less than 2 h, after which equilibration was found to be complete. Excess pentane was evaporated with a gentle stream of nitrogen followed by evacuation to 10^{-4} Torr. Adventitious oxygen could be eliminated by displacement with N_2 after five successive evacuation–nitrogen addition–equilibration cycles. Irradiation of the evacuated zeolite samples was carried out for 60 min in continuously rotating Pyrex tubes with the filtered output (313 nm) of a medium-pressure Hanovia lamp. Overnight extraction with 20 mL of CH_2Cl_2 resulted in adequate (>85%) recovery yields. Quantitative product analysis by GC was achieved after evaporation and dissolution of the extracted photolyzate in 0.5 mL of diethyl ether containing a known amount of hexadecane, which was used as an internal standard. Cage effects were determined by GC/MS analyses with an HP 5890 gas chromatograph connected to an HP 5988 mass selective detector and an HP 9216 workstation. Experiments at -20 °C were carried out by maintaining the photolysis tubes immersed in a Neslab Cryocool thermostated methanol bath with irradiation times of 2 h. The ^{13}C NMR spectrum of the NaX/DBK sample was measured in a Bruker AF 250 instrument equipped with a WP 250SY amplifier from IBM Instruments. The spectrum was obtained with single pulse excitation and high power decoupling after 25 K scans acquired with a 2-s recycle time.

Results

Loading of DBK in NaX. The adsorption of DBK-d_5 in NaX was found to occur relatively fast with equilibrium being reached typically within 2 h as shown by representative kinetic uptake experiments (Figure 1). No significant differences could be found with samples loaded with DBK-d_5 or with samples with natural isotopic abundance. The maximum uptake of ~6.5 mg of DBK in 40 mg of dry zeolite corresponds to a maximum loading of ca. 15% w/w (Figure 2). Langmuir analysis of the presaturation portion of the adsorption data, however, provides the best fit for a maximum value of 13 mg of DBK for 40 mg of dry zeolite, which corresponds to a maximum uptake of ~30% w/w. The deviation from such a value, however, becomes readily evident as the higher

(10) Turro, N. J.; Weed, G. C. *J. Am. Chem. Soc.* **1983**, *105*, 1861.
(11) (a) Lechert, H.; Wittern, K.-P. *Ber. Bunsen-Ges. Phys. Chem.* **1978**, *82*, 1054. (b) de Mallmann, A.; Barthomauf, D. *Zeolites* **1988**, *8*, 292.

Figure 1. Time evolution of the uptake of DBK from a pentane solution containing 10% w/w, showing saturation equilibrium at ca. 8% w/w within ~60 min.

Figure 2. Adsorption isotherm of DBK-d_5 from pentane solution (in 40 mg NaX).

loading values (~10–15%) are approached. It is interesting to compare this value with the maximum equilibrium uptake value of 33% w/w determined in the case of water.[1] The maximum loading occupancy, defined as the number of DBK molecules per supercage, was calculated to be 1.4. Intuitive insights can be obtained if we compare this value with the maximum of ~4–5 molecules per supercage reported in the case of benzene.[11] The average location of the DBK molecules in the zeolite internal structure is not known at the present time. The ^{13}C NMR spectrum of a representative sample containing 10% w/w DBK (occupancy = 0.8) indicates no spectral heterogeneity, which could be due to site or molecular-structural distribution of the ketone (Figure 3). The spectrum obtained in the zeolite is in fact much like that observed in $CHCl_3$ solution (top spectrum). A single

Figure 3. Solid state ^{13}C NMR spectrum of a sample containing 10% w/w DBK in NaX (0.77 molecule/supercage). Spectrum obtained with high-power decoupling.
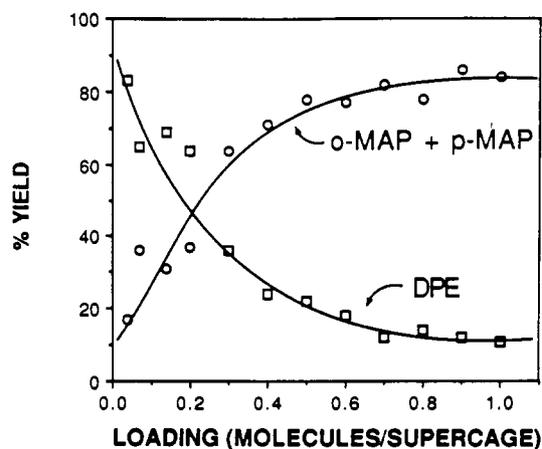

Figure 4. Relative yields of DPE and rearranged products (RP) given by the sum of o-MAP and p-MAP as a function of loading of DBK in NaX.

resonance for each of the six isotropic-carbon signals is observed at chemical shifts within ca. 2 ppm from those observed in solution. The simplicity of the spectrum clearly suggests that possible sources of spectral heterogeneity may be averaged within the time scale of the NMR experiment. The mobility of DBK within the zeolite was further indicated by a spectrum collected under similar conditions but with a static sample. The fact that relatively narrow (~400 Hz) resonances are obtained for every signal group (Ar, $-CH_2-$, and CO) indicates a relatively free molecular motion, where both chemical shift anisotropy and heteronuclear dipolar interactions are averaged by relatively fast molecular motions.

Photochemistry of DBK in NaX as a Function of Loading. Samples of DBK-d_5 in NaX with occupancy values ranging between 0.04 and 1.0 were photolyzed. As in previous studies,[5,6] three different products were formed and identified (Scheme I) by GC coinjection with the authentic samples as diphenylethane (DPE-d_0,-d_5, and -d_{10}), o-methyl-β-phenylacetophenone (o-MAP-d_5), and p-methyl-β-phenylacetophenone (p-MAP-d_5). The relative yields of formation of these products, as summarized in Figures 4 and 5, depend in a rather impressive manner on the loading of DBK-d_5 in each sample. Figure 4 depicts the relative yields of DPE versus the sum of o-MAP and p-MAP, together referred to as rearranged products (RP). In Figure 5, variations on the yields of the two rearranged products (o-MAP and p-MAP) are shown as a function of starting material occupancy. Concomitant analysis of the cage effect on the formation of DPE, computed from GC/MS product analysis, gave the results shown in Figure 6. The cage-effect values plotted in the figure were arrived at by using the relative yields of DPE, DPE-d_5, and DPE-d_{10} and by application of the usual cage-effect relationship:[12]

cage effect = {[DPE-d_5 –

(DPE + DPE-d_{10})]/(DPE-d_5 + DPE + DPE-d_{10})} × 100
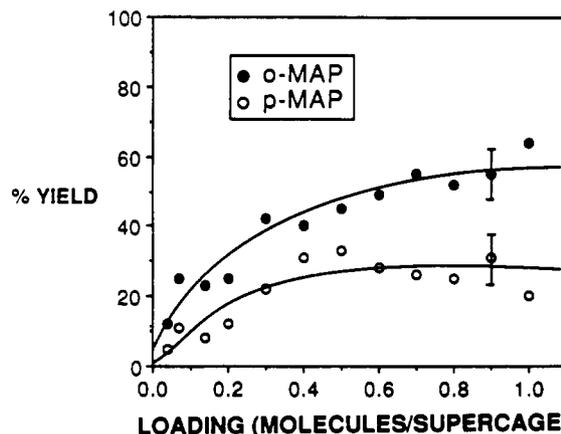
Figure 5. Relative yields of o-MAP and p-MAP as a function of loading of DBK in NaX.
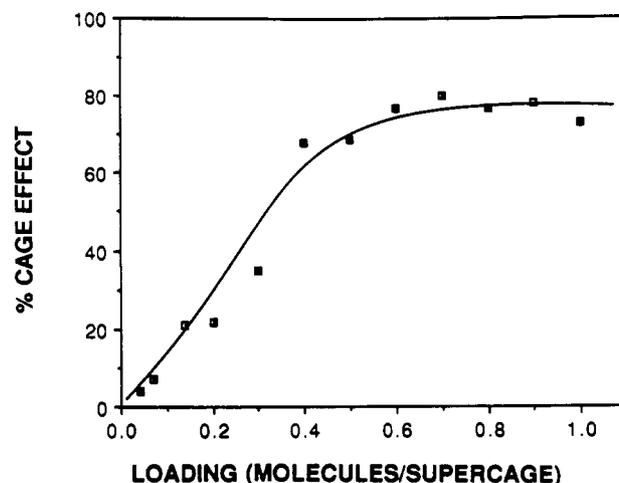
Figure 6. Variations in the cage effect of DPE as function of loading in NaX.

Effect of Oxygen Scavenging on the Photochemistry of DBK in NaX. Over the course of several photolysis experiments it was observed that the yields of products were rather susceptible to the deoxygenation procedure. The formation of benzaldehyde as an alternative reaction product was observed in several instances. Complete deoxygenation, as evidenced by the absence of benzaldehyde, could only be achieved by displacement with nitrogen after five cycles consisting of evacuation (10^{-4} Torr) followed by equilibration with N_2 at atmospheric pressure. Incomplete deoxygenation had the effect of enhancing the formation of benzaldehyde by oxidation of the benzyl radicals, primarily at the expense of the yields of DPE. Although the formation of benzaldehyde could be unambiguously established by GC analysis, quantitative evaluations turned out to be difficult to obtain under our experimental conditions, probably due to further oxidation of benzaldehyde to give benzoic acid. The results from a typical experiment where samples of DBK/NaX were photolyzed after a single evacuation treatment at 10^{-4} Torr, which results in the presence of residual oxygen, are shown in Figure 7. The first striking observation comes from the fact that there is a greatly reduced variation range in the product yields and cage effect with respect to the amount of ketone loaded in the zeolite samples. Notably, the cage effect values remained very high (90–95%) and relatively constant between occupancy values of 0.05 and 0.8. The yields of diphenylethane were found to remain surprisingly low (10–20%), even at occupancy values as low as 0.05. The yields of rearranged products, in contrast, remained high at all loading values with a clear and significant preference for the formation

---

(12) (a) Koening, T.; Fisher, H. In *Free Radicals*; Kochi, J., Ed.; Wiley: New York, 1973; p 157. (b) Sheldon, R.; Kochi, J. *J. Am. Chem. Soc.* **1970**, *92*, 4395.

Diffusion and Percolation of Radical Pairs

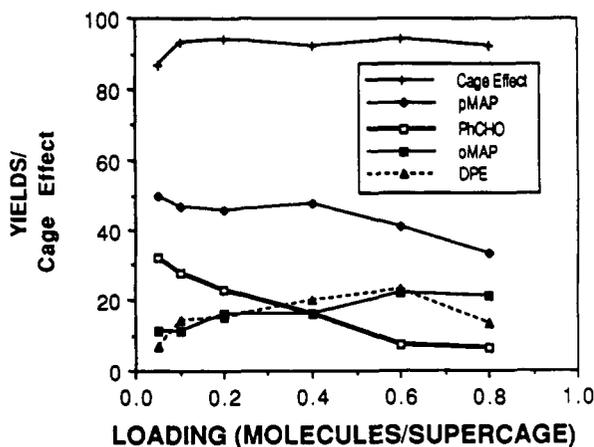*J. Am. Chem. Soc., Vol. 113, No. 16, 1991* 6215

Figure 7. Variations in the product yields and cage effect in the photochemistry of DBK in NaX as a function of loading in the presence of residual oxygen.
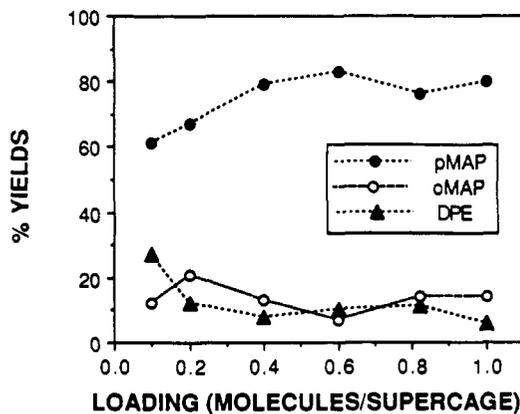

Figure 8. Variations in the product yield and cage effects in the photochemistry of DBK in NaX as a function of loading at -20 °C. Cage effect values consistently larger than 90% were observed at all loadings.

Supercage:
Vertex in Diamond
Structure

Zeolite NaX:
Diamond Structure

Figure 9. (a) Schematic representation of the supercage in the faujasite zeolites. (b) The connectivity between supercages in the faujasite zeolites is equivalent to that of the carbon atoms in diamond. The vertices represent the supercages and the edges represent the interconnecting channels or windows. The relative dimensions are distorted for the purpose of clarity.

of the para coupling product (*p*-MAP). It was observed qualitatively that the yields of benzaldehyde increased systematically toward lower occupancy values. It was assumed in Figure 7 that the formation benzaldehyde or other oxidation products, i.e. benzoic acid, accounts for the material missing after consideration of the yields of DPE, *o*-MAP, and *p*-MAP.

Photochemistry of DBK in NaX as a Function of Loading at -20 °C. Lowering the temperature to -20 °C, similar to the trapping of radicals with an oxygen scavenger, had the effect of decreasing the sensitivity of the product ratio to changes in loading with occupancies between 0.1 and 1.0 (Figure 8). In contrast to photolysis at room temperature (Figure 4), the yields of DPE were found to be low, and within a rather restricted range of ~5-30%. The variation in the yield of isomers at -20 °C was also small and ranged from 73 to 94%. The yields of ketone isomers at the initial loading values turned out to be much larger at low temperature (~73% at 0.1 occupancy in Figure 8) as compared with those obtained at 20 °C (~10% at 0.05 occupancy in Figure 4). The dynamic range of the changes in the yields of rearranged products as a function of loading at the two temperatures was also found to differ substantially, being ~20% at -20 °C (Figure 8) and ~70% at 20 °C (Figure 4). Further differences were found in the relative yields of products of coupling of the primary radical pair, where the ratio *p*-MAP/*o*-MAP changes from 4.0 to 0.5 as the temperature is changed from -20 to 20 °C. The cage effect, in contrast, turned out to be the least sensitive parameter at -20 °C as cage effects greater than 95% were observed at all loading values (Figure 8).

Discussion

The zeolite selected for the present study, NaX, is a member of the family of the faujasites. Its internal topology is constituted by a network of interconnected and nearly spherical cavities (~13
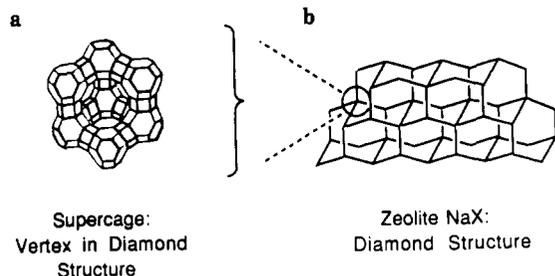
Å inner diameter) known as supercages (Figure 9a). The faujasite supercages possess one of the largest internal void volumes (ca. 822 Å^3), which is accessible to relatively large molecules of photochemical interest such as DBK. The composition of NaX is characterized by having relatively large amounts of aluminum (ratio Si/Al = 1.2). Sodium cations, as implied by the designation NaX, compensate the negatively charged tetravalent aluminum atoms. Previous studies on cation-exchanged MX zeolites (M = Li, Na, K, Rb, and Cs) have suggested an important role of the cations in determining the photochemistry of DBK, mainly by inducing modifications on the size of the available reaction space.[6] The apertures of the channels connecting close-neighboring supercages in the zeolite NaX have diameters of ~7.4 Å and permit the access and traffic of the adsorbate molecules. The size of the supercages, as mentioned before, depends on the nature of the counter-balancing cations.[1] Each supercage in the structure is interconnected to four others in a tetrahedrally disposed arrangement with a connectivity similar to that found in the carbon atoms in the structure of diamond. In the schematic representation of Figure 9b, the vertices of the diamond-like structure represent the supercages, while the edges represent the interconnecting channels. Diffusion in the faujasite structure is on the average equally allowed in all four directions from every supercage, and long-range intracrystalline transport may effectively occur in three dimensions.

The three-dimensional connectivity and the large pore diameter of the intracrystalline spaces in NaX are reflected in the relatively fast uptake of DBK (Figure 1). The maximum loading value of ~1.4 molecules/supercage (Figure 2) indicates a favorable adsorption equilibrium constant and probably an ability to optimize the intracrystalline spaces. It is not known whether occupancy values slightly larger than one molecule per supercage result from double occupancies or from arrangements involving the use of the space available in the interconnecting cylindrical channels. In any case, for the present study and in an attempt to facilitate the interpretation of the photochemical results, occupancy values were kept below 1 molecule/supercage.

The variations in the product ratio (DPE and RP in Figure 4, and *o*-MAP/*p*-MAP in Figure 5) and in the cage effect (Figure 6) as a function of loading can be understood after careful consideration of the reaction mechanism and the role played by loading in changing the properties of the environment. It has been commonly accepted that the product distribution and cage effect observed from DBK depend on the dynamics of the radical pairs as determined by their medium.[9,13] The paradigm for the photolysis of DBK is shown in Scheme II. Local and global spaces, given by the supercage sites and by the extended zeolite diffusion lattices, respectively, have been considered and represented in Scheme II along with pathways involving radical escape and re-encounter. The initial step involves the absorption of a UV photon, which results in the formation of a triplet primary radical pair ^{3}[ACO• •B] after intersystem crossing and an α-cleavage

(13) (a) Engel, P. S. *J. Am. Chem. Soc.* **1970**, *92*, 6074. (b) Robins, W. K.; Eastman, R. *J. Am. Chem. Soc.* **1970**, *92*, 6076.

Scheme II
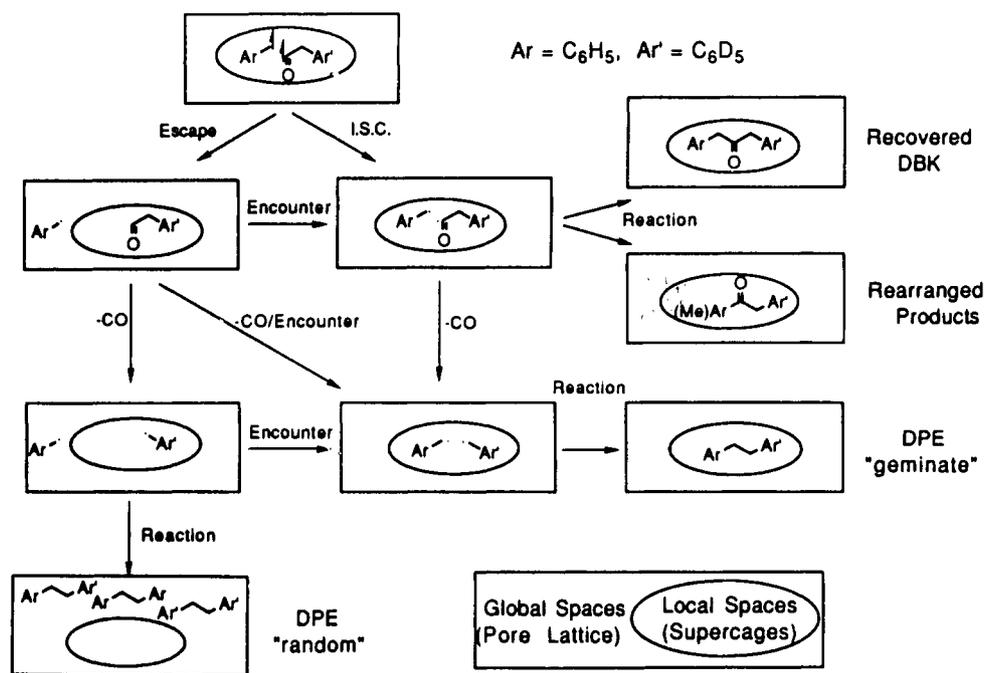
reaction.[13] The fate of the triplet radical pair is determined by the probability of escape from the local supercage environments. Intracage intersystem crossing and primary recombination may occur to give rearranged ketone products (o-MAP and p-MAP) and recovered starting material (DBK). Separation of the radical pair, on the other hand, gives an opportunity for decarbonylation to occur to generate the secondary radical pair, [A$^{\bullet}$ $^{\bullet}$B]. It has been shown that decarbonylation of the primary radical pair in solution occurs within about 100 ns.[15] This value gives an approximate limit for the time required by the triplet primary radical pair to intersystem cross and recombine following an alternative route to rearranged products and recovered DBK. If decarbonylation occurs prior to recombination of the primary radical pair, the secondary radical pair may recombine and re-encounter to give "cage effect" products, or randomize in the global space to give random DPE products.

The local and global environments in the zeolite are structurally restricted analogues of the dynamic primary and secondary solvent cages discussed by Noyes and advanced by Franck and Rabinowitch in liquid media.[14] The local environment of the supercages has the dimensions required to contain the radical pair within molecular-diameter distances and fulfills the conditions for a self-sustained primary cage. Separation of the radical pair beyond molecular-diameter distances occurs only after escape of one or both fragments from the local environment. The escape and recombination probabilities in the zeolite are determined by the global topology as determined both by the structure of the lattice and by the occupancy of the neighboring sites. The average separation of the primary radical pair at any given time within its lifetime should be dictated by the rate of escape from the local environment and by the rate of intracrystalline diffusion in the zeolite lattice.

At low loading values, the average number of empty sites surrounding a reacting DBK molecule and the average number of escape routes are large (Figure 10a). The occupancy value of the reactant in the zeolite may be thought of in terms of *the density of the global environment*, which is expected to affect the
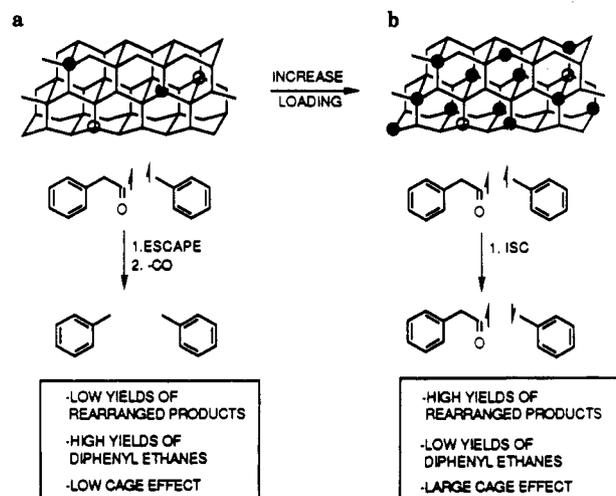

Figure 10. Representation of the supercage occupancy at (a) low loading and (b) high loading values and its influence on the reaction alternatives of the primary and secondary radical pairs. Ground- and excited-state DBK molecules are represented with filled and empty circles, respectively.

re-encounter probability when escape from the local cages is relatively fast, and the primary radical pair has an opportunity to explore the empty supercages in the surrounding global space.[14] It is expected that the benzyl radicals (PhCH$_2^{\bullet}$), without a polar carbonyl group and with a relatively smaller size, may diffuse at a faster rate and explore the environment, while the larger and more polar phenylacetyl radicals (PhCH$_2$CO$^{\bullet}$) remain close to the original reaction site. The rate of intracrystalline diffusion of the benzyl radical (D) may be approximated by that of toluene, which is known to be $\sim 10^{-10}$ m^2 s^{-1}.[16] If we assume a random walk model[17] with a diffusion coefficient given by $D = u^2/6t$, we can calculate that the time for hops of length $u \approx 15$ Å, an approximate intersupercage distance, is $t \approx 3.8 \times 10^{-9}$ s. From

(14) (a) Frank, J.; Rabinowitch, E. *Trans. Faraday Soc.* **1934**, *30*, 120. (b) Rabinowitch, E.; Wood, W. *Trans. Faraday Soc.* **1936**, *32*, 1381. (c) Noyes, R. M. *J. Am. Chem. Soc.* **1955**, *77*, 2042. (d) Noyes, R. M. *J. Am. Chem. Soc.* **1956**, *78*, 5486.

(15) (a) Lunazzi, L.; Ingold, K. U.; Scaiano, J. C. *J. Phys. Chem.* **1983**, *87*, 529. (b) Gould, I. R.; Baretz, B. H.; Turro, N. J. *J. Phys. Chem.* **1983**, *87*, 531. (c) Turro, N. J.; Gould, I. R.; Baretz, B. H. *J. Phys. Chem.* **1987**, *91*, 925.

(16) It should be pointed out that the intracrystalline diffusion coefficient of toluene in NaX is dependent on loading: (a) Germanus, A.; Kärger, J.; Pfeifer, H. *Zeolites* **1984**, *4*, 188. (b) Germanus, A.; Kärger, J.; Pfeifer, H.; Samulevic, N. N.; Zdanov, S. P. *Zeolites* **1985**, *5*, 91.

(17) Heifer, R.; Orbach, R. In *Dynamical Processes in Condensed Molecular Systems*; Klafter, J., Jortner, J., Blumen, A., Eds.; World Scientific: Teaneck, NJ, 1989.

this value we may propose that a chaotically moving benzyl radical may explore as many as 25 supercages within the lifetime of the primary radical pair, i.e. before decarbonylation occurs ($\sim$100 ns). *The probability of the radical returning to the geminate site before 100 ns or after about as many as 25 random hops should be very small in a four-coordinated zeolite lattice with free-molecular traffic.* At low loading values, or under conditions of a low global density, the phenylacetyl radical should escape and decarbonylate to give rise to the second benzyl radical. At high loadings, on the other hand, the number of escape routes and the space available to the primary radical pair become increasingly smaller (Figure 10b). A secondary *global cage*, analogous to that in the model of Noyes, Frank, and Rabinowitch,[14] results from the collective influence of the molecules occupying the surroundings of the radical pair. A limiting situation would be one where every supercage is occupied by one (or more) DBK molecule(s). The triplet primary radical pair should have now a greater probability of intersystem crossing to the singlet state, $^1[ACO^{\bullet\bullet}B]$, and recombining before losing CO and giving rise to the secondary radical pair, $[A^{\bullet\bullet}B]$. In agreement with this explanation, high yields of rearranged products are observed at the high occupancy values.

The above model is consistent with the fact that the yields of rearranged products are low at low loadings when most of the primary radical pairs find their way into decarbonylation products (DPE). Such an explanation is also consistent with the low cage-effect values of DPE observed at low loadings, which indicate a high probability of randomization of the secondary radical pairs in the global intracrystalline spaces. Little or no cage effect at low loadings clearly indicates a relatively inefficient primary cage by the local (supercage) environment. The cooperative action of neighboring molecules at increasing loading values, on the other hand, indicates an increasingly more efficient secondary cage from the global environment. A point of interest comes from the fact that the limiting cage-effect value at loadings higher than $\sim$0.6 is only $\sim$75%, which is somewhat smaller than the possible maximum of 100%. We interpret this result in terms of reactions occurring near the external zeolite surfaces that, lacking the restrictions of the intracrystalline spaces, allow for rapid diffusion and radical randomization.

Another interesting and independent reactivity parameter comes from the relative yields of the rearranged products. While the error in their yields is somewhat larger, it is observed that the yields of formation of the two coupling products varies substantially as the loading values are changed. Notably, *o*-MAP is preferred over *p*-MAP as the loading of DBK is increased at room temperature. This result suggests that reaction to give rearranged products may occur by taking advantage of diffusion, intersystem crossing, and forced return of the radical pair. This mechanism is expected to become more important at higher ketone loadings. Such an explanation may imply that the yields of rearranged products would be determined both by recombination statistics and by steric encumbrance at increasing loading values. Interestingly, the formation of *p*-MAP is slightly favored at low loading values where the influence on primary recombination can be attributed to the local spaces. The formation of *o*-MAP, occurring by coupling of the phenylacetyl radical at the two ortho positions of the benzyl radical, may take advantage of escape and recombination steps. It is in fact shown in Figure 4 that the relative yields of *o*-MAP and *p*-MAP tend to a 2:1 ratio as the occupancy values are increased.

An estimation of the restricting abilities of the local supercage sites and the global zeolite spaces can be obtained from results at different occupancy values. While care must be taken regarding the probability of having preferential occupancy of activated or defect sites, results extrapolated to zero percent loading can be interpreted in terms of local effects. The formation of *o*-MAP and *p*-MAP in yields of $\sim$10% at low loading values suggests that the supercages of NaX are able to impose escape restrictions on the primary radical pair. The low cage-effect values ($\sim$0%) on the recombination of the secondary radical pair, on the other hand, indicate the inefficiency of the local sites in keeping geminate

benzyl radicals together. The probability of having different sites imposing different reaction pathways should also be considered. Interestingly, the properties of the global spaces need to be described as a function of loading.

The size of the space able to determine the dynamics of the radical pairs depends on the occupancy values and should be determined by collective statistical phenomena.[18] The internal zeolite spaces constitute a regular 3-dimensional hypercubic lattice. If a random reactant distribution and a negligible probability for double supercage occupancies are assumed, the average size of the global empty spaces may be described by percolation theory.[19] The dynamics of the DBK-derived radical pairs represent a physical example of the ant in the labyrinth model proposed by de Gennes.[20] However, a further assumption is needed in order to apply the percolation model. The rate of diffusion of DBK and $PhCH_2CO$ should be much smaller than the rate of diffusion of the benzyl-radical random walkers, i.e. the rate of change of the "labyrinth", given by the rate of diffusion of DBK, should be smaller than the rate at which the "ants" (benzyl radicals) explore it.[17,21]

There are three events of interest in the present system that determine the outcome of the reaction: (a) intersystem crossing and recombination of the primary radical pair, (b) decarbonylation and recombination of the secondary radical pair, and (c) escape of the radical partners from an isolated (either local or global) site. These events are determined by the size and connectivity of the global spaces. At loadings approaching an occupancy of one DBK molecule per supercage, there are no empty sites and the probability of any site being empty, $\langle e \rangle$, is $\langle e \rangle = 0$. As the occupancy values are decreased and the number of empty sites increases ($\langle e \rangle > 0$), the size of the global spaces also increases on the average, giving rise to clusters of empty sites or "empty pockets". Percolation theory predicts that at the percolation threshold value, when the number of empty sites reaches a critical value, $\langle e \rangle$, empty pockets will be formed that extend throughout the entire zeolite lattice.[19] The percolation threshold also determines the occurrence of a number of critical transitions such as those given by the average number of clusters, the density of sites in the infinite cluster, and the mean cluster size. It is precisely the latter quantity that is of particular relevance to the escape and recombination problem addressed in this investigation. The percolation threshold calculated for the diamond structure in NaX is expected to occur when $\langle e \rangle_c = 0.39$.[19] Experimentally, it is shown in Figures 4–6 that breaks in the product yields and cage effect occur at occupancy levels close to 0.6, implying a concentration of empty sites of $\langle e \rangle \approx 0.4$. This value has an impressive correspondence with the percolation threshold value for the diamond structure of NaX.

The picture emerging from the previous analysis indicates the importance of diffusion and precursor loading and distribution on the dynamics of radical pairs in zeolite media. The effect of oxygen scavengers in the zeolite lattice provides further support for this argument (Figure 7). Notably, the formation of benzaldehyde in the presence of oxygen occurs mostly at the expense of DPE and is accompanied by an increase in the yields of rearranged products. As expected in a diffusion-mediated process, this effect appears to be more important at the lower ketone loadings. Large cage effects with little or no loading dependence imply that benzyl radicals exploring the global pore lattice are

(18) (a) Anacker, L. W.; Kopelman, R. *Phys. Rev. Lett.* **1987**, *58*, 291. (b) Zumofen, G.; Blumen, A.; Klafter, J. *J. Chem. Phys.* **1985**, *82*, 3198. (c) Walsh, C. A.; Kozak, J. J. *Phys. Rev.* **1982**, *B26*, 4166. (d) Politowicz, P. A.; Kozak, J. J. *Mol. Phys.* **1987**, *62*, 939.

(19) Stauffer, D. *Introduction to Percolation Theory*; Taylor and Francis: London, 1985.

(20) (a) de Gennes, P. G. *Recherche* **1976**, *7*, 919. (b) Stauffer, D. *Phys. Rev.* **1977**, *54*, 1. (c) Gefen, Y.; Aharony, A.; Alexander, S. *Phys. Rev.* **1983**, *53*, 77.

(21) An alternative approach to the understanding of the loading-dependence reaction profiles may be based on the consideration of the mean walk length of the radicals, $\langle n \rangle$, and its dependence on the trapping probability, s ($s|0 < s < 1$).[18] Uncorrelated radicals can be viewed as traps, while geminate radical partners can be looked at as targets. We acknowledge a referee for valuable suggestions.

likely to encounter oxygen and form the benzaldehyde. The effect of oxygen, however, extends beyond that of a simple radical scavenger. An increase in the yields of primary recombination products, primarily of *p*-MAP, appears to indicate that most of the reaction occurs at the local supercage sites. It can be speculated on whether the paramagnetic oxygen molecules induce an enhanced rate of intersystem crossing of the radical pair. Such an effect is well documented and has been discussed by Scaiano[22] and others.[23] Oxygen, presumably being a faster random walker, may be able to induce intersystem crossing of the radical pair as it approaches the local supercage sites.

Finally, the result of carrying out the reaction at –20 °C also supports the percolation model. It is expected that a decrease in temperature should decrease the diffusion coefficient of all the species in the zeolite media. Low temperatures would therefore be expected to increase the role of local effects at all loadings as the mobility of the reaction intermediates is highly reduced. Such expectations are observed as the loading dependence of the product yields and the cage effect are substantially reduced (Figure 8). The yields of rearranged products, in relation to the results at room temperature, are increased substantially (70% to 90%) at all

loadings. The yields of DPE indicate relatively small variations (30% to 5%), while consistently large cage effects are observed at all loadings (90% to 95%). A striking observation, which confirms the preferential formation of *p*-MAP at the local reaction sites, comes from the fact that the highest yields of this product (60–80%) are observed under these "diffusion-frozen" conditions. This interpretation, however, does not take into account temperature-induced changes in the rates of reaction.

Conclusions

The importance of loading on the dynamics of the radicals derived from the photolysis of DBK-d_5 in NaX has been demonstrated. The results presented here suggest that the effect of additives in the dynamics of intrazeolite reactions may be explained with the consideration of local and global space effects and by use of percolation theory. It is also suggested that the relative diffusion rates of the reactants and reaction intermediates should be taken into account in order to consider the applicability of a percolation model. Further work studying the effect of loading of various aromatic coadsorbates with different diffusion coefficients in zeolite media is currently under progress.

(22) Scaiano, J. C. *Tetrahedron* **1982**, *38*, 819.
(23) Kuz'min, V. A.; Levin, P. P. *Bull. Acad. Sci. USSR, Div. Chem. Sci. (Engl. Transl.)* **1989**, 1291.

Use of Ionization Potentials, Electron Affinities, and Singlet–Triplet Excitation Energies for the Estimation of Reaction Barriers

Vernon D. Parker,* Kishan L. Handoo,[1] and Björn Reitstöen

Contribution from the Department of Chemistry and Biochemistry, Utah State University, Logan, Utah 84322-0300. Received October 5, 1990. Revised Manuscript Received April 6, 1991

Abstract: The use of ionization potentials (I_D), electron affinities (E_A), and singlet–triplet excitation energies ($\Delta E_{ST}(\pi\pi^*)$) to estimate reaction barriers for donor (D)–acceptor (A) combination reactions i has been examined. It is evident from thermochemical cycles that these quantities are not a complete description of the energetics of the excitation of reactant ground-state configuration 1 to the first excited-state configuration 2. The association constants of ground state (K°) and excited state (K^*) reactants must also be taken into account. Including a term for the latter gives rise to eq ii, in which f is a fraction and

$$D/A \rightarrow D^+ – A^- \qquad\qquad (i)$$

$$\underset{\mathbf{1}}{D \colon A} \qquad \underset{\mathbf{2}}{{}^+D^{\cdot}{}^{\cdot}A^-}$$

$$\Delta E_{act} = f[(I_D - E_A) - RT \ln (K^*/K^\circ)_{DA}] - B \qquad\qquad (ii)$$

B is the avoided crossing parameter, for the estimation of the reaction barrier using the state correlation diagram (SCD) analysis. It is concluded that linear correlations of ΔE_{act} vs $I_D - E_A$ are not expected to provide either f or B. The energies of excitation of **1** to **2** in acetonitrile, where D is an aromatic compound and A is tropylium ion, were observed to be lower than values calculated from $I_D - E_A$ by as much as 13–23 kcal/mol, indicating the need for a significant correction due to the $RT \ln (K^*/K^\circ)_{DA}$ term. The consequences of the association equilibria of ground-state and excited-state complexes on excitation energies and reaction barriers are discussed for free-radical phenylation of aromatic compounds.

Introduction

Ionization potentials, electron affinities, and singlet–triplet excitation energies are frequently referred to in the discussion of reaction barriers.[2-7] When used to estimate barriers of bimo-

lecular reactions, it is often necessary to combine two or more of the quantities corresponding to the two reactants. In doing so, the mutual interactions of the ground-state reactants to form the reactive complex, as well as the corresponding interactions

(1) On leave from the Department of Chemistry, University of Kashmir, India.
(2) Epiotis, N. D.; Shaik, S. S. *J. Am. Chem. Soc.* **1977**, *99*, 4936.
(3) Warshel, A.; Weiss, R. M. *J. Am. Chem. Soc.* **1980**, *102*, 6218.
(4) Shaik, S. S. *J. Org. Chem.* **1987**, *52*, 1563.
(5) Pross, A. *J. Am. Chem. Soc.* **1986**, *108*, 3537.
(6) Buncel, E.; Shaik, S. S.; Um, I.-H.; Wolfe, S. *J. Am. Chem. Soc.* **1988**, *110*, 1275.
(7) Shaik, S. S.; Canadell, E. *J. Am. Chem. Soc.* **1990**, *112*, 1446.